Duration and nonlocality of a nucleon-nucleon collision

Klaus Morawetz
Fachbereich Physik, University Rostock, D-18055 Rostock, Germany

Pavel Lipavský and Václav Špička
Institute of Physics, Academy of Sciences, Cukrovarnická 10, 16200 Praha 6, Czech Republic

Nai-Hang Kwong
Physics Department, University of Arizona, Tucson, Arizona 85721
(Received 25 November 1998)

For a set of realistic nucleon-nucleon potentials we evaluate microscopic parameters of binary collisions: time duration of the scattering state, mean distance, and rotation of nucleons during a collision. These parameters enter the kinetic equation as noninstantaneous and nonlocal corrections of the scattering integral, i.e., they can be experimentally tested. Being proportional to off-shell derivatives of the scattering T matrix, noninstantaneous and nonlocal corrections make it possible to compare the off-shell behavior of different potentials in a vicinity of the energy shell. The Bonn one-boson-exchange and Paris potentials are found to yield very close results, while the separable Paris potential differs. [S0556-2813(99)00906-1]

PACS number(s): 21.30.Fe, 24.10.Cn, 05.20.Dd, 25.70.Pq

I. INTRODUCTION

Most realistic studies of heavy ion reactions deal with local and instantaneous binary collisions as they appear in the Boltzmann, or the Boltzmann-Uehling-Uhlenbeck (BUU), equation. The importance of the nonlocal treatment of collisions has been first pointed out by Halbert [1] and Malfliet [2] and more recently also studied by Kortemeyer, Daffin, and Bauer [3]. In these studies, nucleons are treated as hard spheres, i.e., each collision is instantaneous and a distance of nucleons at the instant of collision equals the diameter of the scattering cross section. This is a questionable approximation, a further progress in these studies hence requires evaluating the nonlocal corrections from a microscopic picture.

The first step in this direction was done by Danielewicz and Pratt [4]. They implemented the Beth-Uhlenbeck approach supplemented with the Wigner concept of the collision delay to evaluate virial corrections to the pressure of the nuclear matter. At first glance, the correction discussed by Danielewicz and Pratt is quite different from Refs. [1–3]. Indeed, the hard-sphere collisions are instantaneous and nonlocal while in the Wigner approach all collisions are local but noninstantaneous. A comparison of both concepts is not so straightforward, however. The Wigner collision delay does not describe a duration of collision but provides the best one-parameter fit of the scattered wave in the asymptotic region. In particular, the Wigner collision delay for the collision of hard spheres is nonzero because a particle reflected by a hard-sphere potential arrives at the asymptotic region sooner then it would do in a reference pointlike (local) scattering event. In this way, the Wigner collision delay represents a mixture of the collision duration and a certain approximation of nonlocal corrections. The quantitative comparison of both approaches is possible. Numerical values of the Wigner collision delay, found by Danielewicz and Pratt from the scattering T matrix, differ from the hard-sphere estimate.

A picture of collision, which is nonlocal and noninstantaneous at the same time, has resulted from the Green's function approach to the kinetic equation [5]. As in the Wigner concept, there is a characteristic time Δ_t determined from the scattering T matrix. The time Δ_t vanishes in the limit of hard spheres what shows that it can be interpreted as a duration of collision.[1] The nonlocal corrections, also determined from the T matrix, are treated separately. In the limit of hard spheres they yield the displacement which equals the diameter of the hard sphere. The nonlocal and noninstantaneous theory furnishes us with a link between both approaches discussed above. If one neglects collisions on the time scale of the collision duration, the collision found in Ref. [5] can be recast into an instantaneous and nonlocal event. This approximation was used in [6] as a convenient tool to incorporate the collision duration together with nonlocal corrections into realistic simulations of heavy ion reactions. Similarly, the Wigner concept is achieved if one neglects the angular momentum of colliding particles.

In this paper we discuss numerical values of the collision duration, the hard-sphere-type displacement of particles, and the displacement related to the angular momentum. Following Ref. [5], we evaluate these parameters of nonlocal and noninstantaneous corrections from the scattering T matrix. The presented results show that the Wigner collision delay is a good approximation at the low-energy region where the model of hard spheres is not adequate. For higher energies, the angular and energy dependencies of the nonlocal and

[1] In Refs. [5] and [6] the terms collision duration and collision delay are treated as equivalent. Here we use the collision delay exclusively for the Wigner concept while the collision duration is used for the concept of Ref. [5].

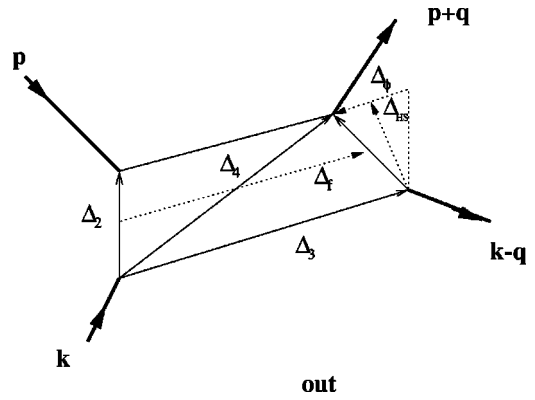

FIG. 1. The nonlocal binary collision.

noninstantaneous corrections are too complicated to be captured by a simple model.

Numerical values of nonlocal and noninstantaneous corrections depend on the interaction potential one employs. Although this dependence is not dramatic, it is stronger than the dependence of the differential cross section. Since values of corrections can, at least in principle, be inferred from heavy ion reactions, they promise a supplementary test of interaction potentials.

II. PARAMETERS OF NONLOCAL COLLISIONS

A picture of the nonlocal collision is outlined in Fig. 1. It presents an event in which the particle a of the momentum k scatters with the particle b of the momentum p loosing the momentum q, i.e., a ends with $k-q$ and b ends with $p+q$. At the beginning of the collision, these particles are displaced from each other by Δ_2. Placing the particle a into the initial of coordinate, we associate Δ_2 with the initial position of particle b. During the collision both particles move, accordingly, at the end of the collision the particle a has the position Δ_3 and the particle b has the position Δ_4.

A. Elementary displacements

The displacements $\Delta_{2,3,4}$ can be expressed in terms of quantities with a more transparent physical meaning. During the collision lasting for Δ_t, the center of mass of the colliding pair flies over a distance

$$\Delta_f=\frac{k+p}{2m}\Delta_t, \tag{1}$$

where we assume that the particles have equal masses m. Since the colliding pair has a nonzero angular momentum, during Δ_t they rotate around each other so that their relative displacement changes by $2\Delta_\phi$. The last independent vector can be selected from the symmetry. The flight Δ_f and the rotation Δ_ϕ reverse their orientations under time inversion. It is advantageous to complement them with the mean of initial and final distance $\Delta_{\rm HS}$ seen in Fig. 1, which is invariant under time inversion. The positions of the particles are linked with the elementary displacements by relations evident from Fig. 1

$$\begin{aligned}2\Delta_\phi&=\Delta_4-\Delta_3-\Delta_2,\\ 2\Delta_{\rm HS}&=\Delta_4-\Delta_3+\Delta_2,\\ 2\Delta_f&=\Delta_4+\Delta_3-\Delta_2.\end{aligned} \tag{2}$$

The direction of Δ_f is identical to the center-of-mass velocity, see Eq. (1). For central forces, both remaining displacements lay in the collision plane. The direction of $\Delta_{\rm HS}$ is then identical to the direction of the transferred momentum q. We note that in the limit of hard spheres, $|\Delta_{\rm HS}|$ equals the sphere diameter while the other Δ's vanish. The rotational displacement Δ_ϕ is orthogonal to $\Delta_{\rm HS}$ having the direction of $k-p-q$. Accordingly, only three scalar parameters Δ_t, $|\Delta_{\rm HS}|$, and $|\Delta_\phi|$, are sufficient to characterize the noninstantaneous and nonlocal features of the collision.

B. Collision duration versus delay

As pointed out above, the collision duration differs from the Wigner collision delay. It is profitable to outline why the duration and not the delay is more suitable to describe properties of nucleon-nucleon collisions.

One can observe the collision from two different aspects. First, in the asymptotic region the nonlocal and noninstantaneous corrections are aimed at providing the exact trajectory of the scattered wave packet. From this asymptotic point of view, one of the three above parameters is redundant. Indeed, the displacement in the direction of the outgoing trajectory can be recast into the modified collision duration, which is just the Wigner collision delay. Alternatively, one can extrapolate the incoming and outgoing trajectories so that the collision duration is suppressed and the collision is effectively instantaneous, see Ref. [6].

Second, one can observe a dense system and try to measure what share of nucleons just undergo a collision. This share is given by the so-called correlated density [7]. The correlated density depends on the collision duration but not on the displacements, see Ref. [5]. To cover both aspects, all the three parameters are necessary and the collision duration, not the Wigner collision delay, has to be used.

C. Relation to the T matrix

To evaluate the collision duration and the displacements one needs the retarded T matrix $T(\Omega,k,p,q)$ as a function of the incoming and transferred momenta and an independent energy Ω. The Δ's given by derivatives of the scattering phase shift $\mathrm{Im}\ln T$. According to Ref. [5] the collision duration reads

$$\Delta_t=\mathrm{Im}\frac{1}{T}\frac{\partial T}{\partial\Omega}. \tag{3}$$

Note that one has to evaluate the T matrix out of the energy shell, although only the on-shell value $\Omega=k^2/2m+p^2/2m$, of the collision duration appears as the noninstantaneous correction in the kinetic equation. The on-shell condition is used after taking the derivative. From Eq. (2) and $\Delta_{2,3,4}$ found in Ref. [5] one obtains the hard-sphere and rotational displacements

$$\Delta_{\rm HS}=\mathrm{Im}\frac{1}{2T}\left(\frac{\partial T}{\partial p}-\frac{\partial T}{\partial k}-2\frac{\partial T}{\partial q}\right),$$

$$\Delta_\phi=\mathrm{Im}\frac{1}{2T}\left(\frac{\partial T}{\partial k}-\frac{\partial T}{\partial p}\right). \tag{4}$$

Again, Ω is an independent variable and the on-shell value is taken after derivatives.

III. FREE-SPACE COLLISIONS

Our aim is to evaluate the collision duration Δ_t, the hard-sphere displacement $\Delta_{\rm HS}$, and the rotational displacement Δ_ϕ for a collision of two nucleons in the free space. The translational, rotational and time-reversal symmetries make it possible to express all these quantities in terms of the decomposition into partial waves.

A. Symmetries

Formulas (3) and (4) are expressed in terms of momenta (k,p,q) commonly met in the scattering integral of the kinetic equation. For the numerical evaluation, it is advantageous to rearrange them into the barycentric framework where one can more conveniently handle symmetries of collisions. To this end we write the T matrix as a function of total momentum K, initial relative momentum κ, and final relative momentum κ_f,

$$K=k+p,$$

$$\kappa=\frac{1}{2}(k-p),$$

$$\kappa_f=\frac{1}{2}(k-p)-q. \tag{5}$$

In this representation the hard-sphere and rotational displacements read

$$\Delta_{\rm HS}=-\mathrm{Im}\frac{1}{2T}\left(\frac{\partial T}{\partial \kappa}-\frac{\partial T}{\partial \kappa_f}\right),$$

$$\Delta_\phi=\mathrm{Im}\frac{1}{2T}\left(\frac{\partial T}{\partial \kappa}+\frac{\partial T}{\partial \kappa_f}\right), \tag{6}$$

and the collision duration is defined by Eq. (3).

The nucleon-nucleon interaction includes the tensor forces, therefore the scattering has to be treated with the theory for noncentral forces. To avoid this complication, in the present treatment we will focus on the trace element of the decomposition of the T matrix into singlet and triplet channels. This element obeys the same symmetries as the T matrix of scattering on central forces. To avoid redundant symbols, from now on the T matrix means the approximation by its trace component. This approximation is specified below, see Eq. (13).

The trace element of the T matrix depends only on the relative initial and final kinetic energies measured by $|\kappa|$ and $|\kappa_f|$, respectively, and on the deflection angle θ, given by $\cos\theta=\kappa\kappa_f/|\kappa||\kappa_f|$,

$$T\equiv T\left(\Omega-\frac{K^2}{4m},\cos\theta,|\kappa|,|\kappa_f|\right). \tag{7}$$

The independent energy Ω is reduced by the center-of-mass kinetic energy $K^2/4m$ due to the transformation into the barycentric framework.

Apparently, the T matrix (7) depends on four scalar arguments, therefore there can be at maximum four independent derivatives. This number is reduced to three by the space-reversal and the time-reversal symmetries which require [8]

$$T(\Omega,\cos\theta,|\kappa|,|\kappa_f|)=T(\Omega,\cos\theta,|\kappa_f|,|\kappa|). \tag{8}$$

The displacements are evaluated on the energy shell, where (after taking derivatives) the amplitudes of the initial and the final momenta equal each other, $|\kappa_f|=|\kappa|$. From the symmetry (8) then follows

$$\left.\frac{\partial T(|\kappa|,|\kappa_f|)}{\partial|\kappa_{\rm f}|}\right|_{|\kappa_f|=|\kappa|}=\left.\frac{\partial T(|\kappa|,|\kappa_f|)}{\partial|\kappa|}\right|_{|\kappa_f|=|\kappa|}=\frac{1}{2}\frac{\partial T(|\kappa|,|\kappa|)}{\partial|\kappa|}$$

$$\equiv\frac{1}{2}\frac{\partial T(|\kappa|)}{\partial|\kappa|}. \tag{9}$$

Accordingly, only three of the derivatives are independent, in agreement with three parameters needed to describe the noninstantaneous and nonlocal features of collisions. From now on we use the last form in the second line.

The symmetry determines the direction of displacements. On the energy shell the vector derivatives simplify as

$$\left(\frac{\partial}{\partial\kappa}\pm\frac{\partial}{\partial\kappa_f}\right)T(\cos\theta,|\kappa|,|\kappa_f|)\Big|_{|\kappa_f|=|\kappa|}$$

$$=(\kappa\pm\kappa_f)\left(\frac{1}{2|\kappa|}\frac{\partial}{\partial|\kappa|}-\frac{\cos\theta\mp1}{|\kappa|^2}\frac{\partial}{\partial\cos\theta}\right)T(\cos\theta,|\kappa|). \tag{10}$$

From Eqs. (6) and (10) one can see that the displacements

$$\Delta_{\rm HS}=\overline{\Delta_{\rm HS}}\frac{\kappa-\kappa_f}{|\kappa-\kappa_f|},$$

$$\Delta_\phi=\overline{\Delta_\phi}\frac{\kappa+\kappa_f}{|\kappa+\kappa_f|} \tag{11}$$

follow directions expected from the symmetries. The hard-sphere displacement is parallel to the transferred momentum $q=\kappa-\kappa_f$. The rotational displacement stays in the collision plane and is orthogonal to the transferred momentum. The orthogonality follows from the energy conservation $(\kappa+\kappa_f)(\kappa-\kappa_f)=\kappa^2-\kappa_f^2=0$.

The displacement lengths $\overline{\Delta_\phi}$ and $\overline{\Delta_{\rm HS}}$ are defined by Eq. (11). Their values are easily traced down from Eqs. (6) and (10). Below we provide their explicit forms. We call them lengths to emphasize that they are scalars, they can, however, assume both positive and negative values.

It is noteworthy that for the zero-angle scattering $\theta=0°$ or $\kappa_f=\kappa$, the transfer momentum is zero so that its direction is not defined. The hard-sphere displacement thus cannot be

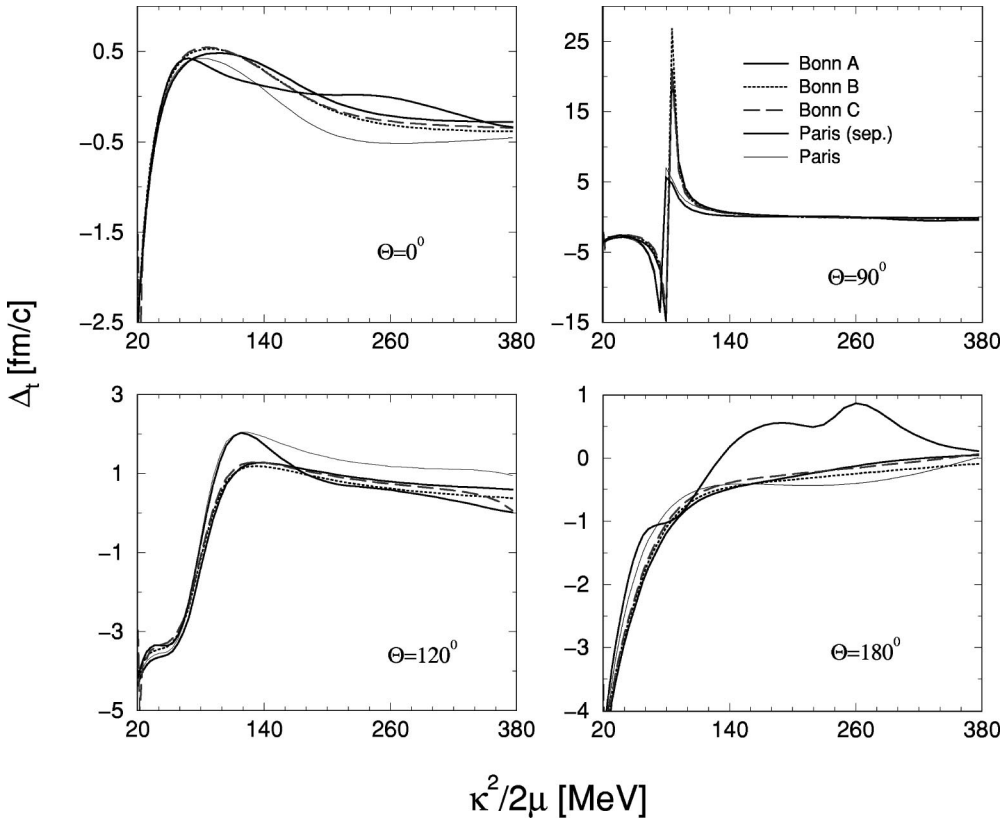

FIG. 2. The collision duration Δ_t as a function of the deflection angle θ and the kinetic energy $|\kappa|^2/m \equiv \kappa^2/2\mu$ in the barycentric coordinate system. A dramatic change from the negative to positive collision duration seen for the perpendicular scattering $\theta = 90°$ at energies about 80 MeV, appears for processes of a vanishing scattering rate. Good agreement is found between results obtained from five different interaction potentials, except for the back scattering $\theta = 180°$ where the separable Paris potential yields appreciably different results from the others.

constructed. This is a peculiarity of the quantum picture of collisions within which the collision plane is determined by the initial and final momenta. Within the classical picture, the collision plane can be determined from the initial momentum and the impact parameter. According to Fig. 1, the hard-sphere displacement then equals to the impact parameter and is perpendicular to the initial momentum. Similarly, for back scattering, $\theta = 180°$ or $\kappa_f = -\kappa$, the direction of the rotational displacement is not defined within the quantum picture. As we will see below, this problem is only academic since both displacements vanish in the questionable cases.

B. Decomposition in partial waves

It remains to evaluate the collision delay and amplitudes of the displacements. To this end we use the decomposition of the spin averaged T matrix into partial waves

$$T(\Omega, \cos\theta, |\kappa|) = \frac{1}{16\pi} \sum_l P_l(\cos\theta) T_l(\Omega, |\kappa|), \quad (12)$$

where P_l is a Legendre polynomial. The coefficients T_l are on the shell $|\kappa_f| = |\kappa|$. They are linked to the usual channel partial T matrices [8]

$$T_l = \sum_{I,S=0,1} \sum_{J=|S-l|}^{S+l} (2J+1)(2I+1) T_{l,l}^{S,I,J} \quad (13)$$

with total spin S, isospin I, and total angular momentum J. Due to summation over projection components m_l, m_s only diagonal elements in l contribute.

Substitution of decomposition (12) into Eqs. (3) and (6) with Eq. (10) yields

$$\Delta_t = \mathrm{Im}\left[\frac{1}{T} \sum_l P_l \frac{\partial T_l}{\partial \Omega}\right],$$

$$\overline{\Delta_{\mathrm{HS}}} = \frac{\sin\theta/2}{|\kappa|} \mathrm{Im}\left[\frac{1}{T} \sum_l P_l' T_l (1+\cos\theta) - |\kappa| P_l T_l'\right],$$

$$\overline{\Delta_\phi} = \frac{\cos\theta/2}{|\kappa|} \mathrm{Im}\left[\frac{1}{T} \sum_l P_l' T_l (1-\cos\theta) + |\kappa| P_l T_l'\right], \quad (14)$$

where $P_l'(z) = (\partial/\partial z) P_l$ is the derivative of the Legendre polynomial and $T_l' = \frac{1}{2}(\partial/\partial|\kappa|) T_l(|\kappa|)$.

Quantum formulas (14) show that the hard-sphere displacement Δ_{HS} is proportional to $\sin\theta/2$ and thus vanishes for the zero angle scattering. Similarly, the rotational displacement Δ_ϕ is proportional to $\cos\theta/2$ so that it vanishes for the back scattering. The undefined directions of the displacements in these cases thus does not cause any problems.

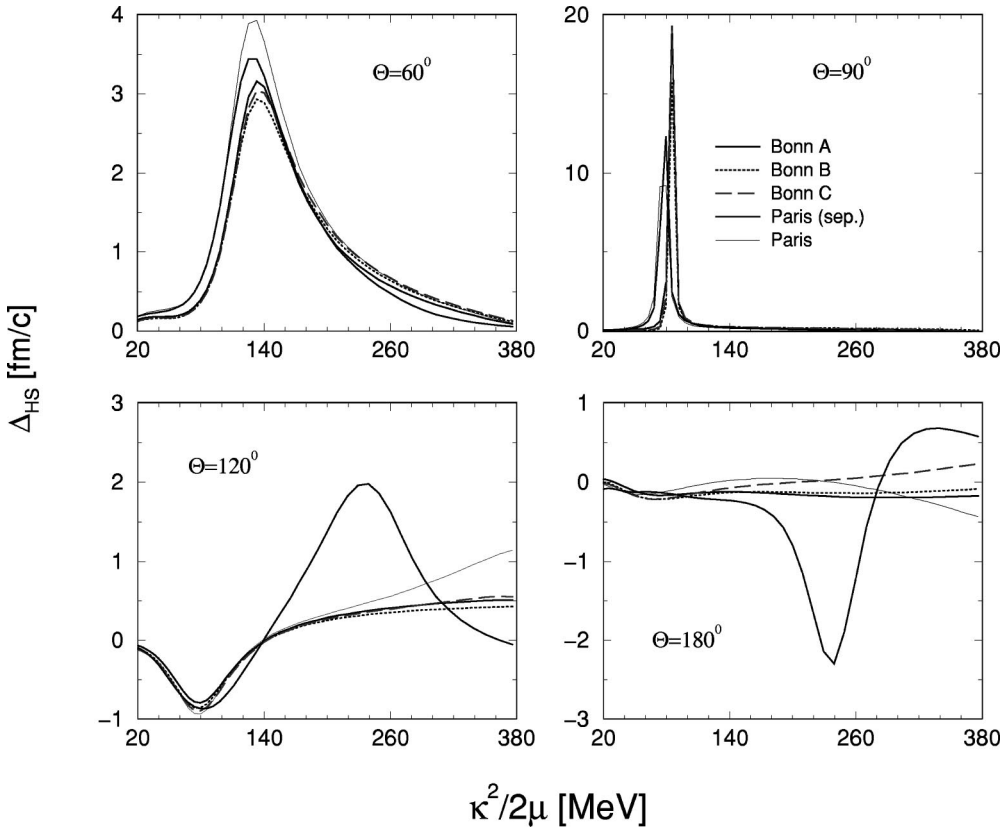

FIG. 3. The hard-sphere displacement $\overline{\Delta_{\rm HS}}$ for conditions identical to Fig. 2. The forward scattering is not included because $\overline{\Delta_{\rm HS}}=0$ for $\theta=0°$. As in Fig. 2, processes corresponding to the singularity seen at $\theta=90°$ and $\kappa^2/2\mu=80$ MeV have a vanishing scattering rate, and the separable approximation leads to serious deviations for large deflection angles $\theta=120°$ and $\theta=180°$.

IV. NUMERICAL RESULTS

Numerical values of the collision duration Δ_t, the hard-sphere displacement $\overline{\Delta_{\rm HS}}$, and the rotational displacement $\overline{\Delta_\phi}$ are shown in Figs. 2–4. They are evaluated from Eq. (14) with the sum over partial waves terminated above D waves but the coupled channels $^3P_2$-$^3F_2$ and $^3D_3$-$^3G_3$, are included along with $^3S_1$-$^3D_1$. We compare results for five approximations of the nucleon-nucleon potential: a set (A–C) of one-Boson-exchange Bonn potentials [9,10], the Paris potential [11], and the separable Paris potential [12].

A. Collision duration

In Fig. 2 we plot the collision duration for different scattering angles versus lab energy. Three features are apparent: (i) at low energies the collision duration reaches large negative values for all deflection angles, (ii) at higher energies the collision duration strongly depends on the deflection angle, and (iii) sharp discontinuities, as the one seen for $\theta=90°$ at energy 80 MeV, might appear.

The large negative values (i) of the collision duration at low energies follow from general properties of the T matrix. The real part $\mathrm{Re}\,T$ is regular for $\Omega\to 0$ while the energy dependence of the imaginary part $\mathrm{Im}\,T$ is proportional to the density of states $\mathrm{Im}\,T\propto\sqrt{\Omega}$. At low energies, the collision duration hence behaves as $\Delta_t\approx(1/\mathrm{Re}\,T)(\partial\,\mathrm{Im}\,T/\partial\Omega)\propto 1/\sqrt{\Omega}$. Using the on-shell condition $\Omega=|\kappa|^2/m$, one can express this singularity as $\Delta_t\propto 1/|\kappa|$. Such a singularity is not dangerous for the kinetic equation since the mean time between collisions also scales with $1/|\kappa|$ being inversely proportional to velocity.

The negative value of the collision duration shows that positions of nucleons are anti-correlated, i.e., it is less likely to find them in a close vicinity than it would be the case in the absence of the interaction. This feature appears also in classical systems, where two particles speed up their motion in the range of their attractive potential passing each other faster than in the absence of forces.

The angular dependence (ii) of the collision duration is surprisingly irregular. The back scattering, $\theta=180°$, reveals monotonic energy dependence of the collision duration. The forward scattering, $\theta=0°$, has a single maximum at 100 MeV. The perpendicular scattering, $\theta=90°$, has a $1/x$ singularity at 80 MeV. Finally, the scattering at $\theta=120°$ has a step at 30 MeV which likely results from a smoothened $1/x$ singularity at 80 MeV.

The strong angular dependence shows that an interference between S,P,D waves plays the important role in the collision duration. For instance, at $\theta=0°$ all Legendre polynomials equal to unity, $P_{0,1,2}=1$, therefore the T matrix reads $T=1/16\pi(T_0+T_1+T_2)$. At $\theta=180°$, $P_{0,2}=1$ and $P_1=-1$, therefore $T=1/16\pi(T_0-T_1+T_2)$. The difference between the collision duration at $\theta=0°$ and $\theta=180°$ thus follows from a different interference of the P wave with the other waves.

The angular dependence reduces at energies below 30 MeV. For this energy, the de Broglie wavelength $\hbar/|\kappa|\sim 1$

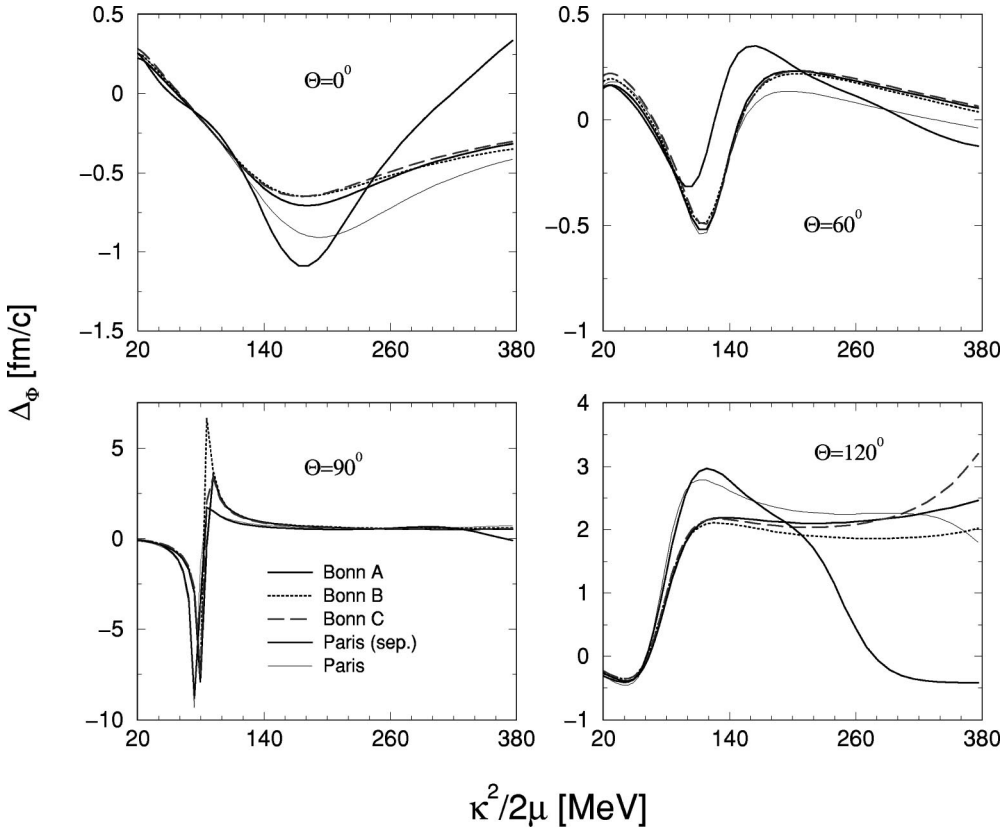

FIG. 4. The rotational displacement $\overline{\Delta_\phi}$ for conditions identical to Fig. 2. The back scattering is not included because $\overline{\Delta_\phi}=0$ for $\theta=180°$. Note similarities with Fig. 2 for deflection angles $\theta=90°$ and $\theta=120°$.

fm is comparable to the range of the interaction potential. With increasing wave length, the interaction potential behaves more and more as a contact potential, therefore the S component of the scattered wave dominates at all angles.

In the $1/x$ discontinuity (iii) at 80 MeV and $\theta=90°$, the collision duration reaches such high values that one might wonder why the instantaneous approximation of the collision works so well. In fact, this type of singularity is not dangerous for kinetic equations, because it appears when the differential cross section vanishes. To see it in more detail, let us write the T matrix. For $\theta=90°$ we have $P_0=1$, $P_1=0$, and $P_2=-\frac{1}{2}$, therefore $T=1/16\pi(T_0-\frac{1}{2}T_2)$. At the energy of 80 MeV the S and D waves destructively interfere and $T\to 0$ while its energy derivative remains finite, $\partial T/\partial\Omega\neq 0$. This causes the $1/x$ discontinuity seen in Δ_t. In the kinetic equation the collision duration enters in a product with the cross section, as a gradient contribution proportional to $|T|^2\Delta_t$. At the point of singularity, $|T|^2\Delta_t\to 0$. It is possible that the $1/x$ discontinuity will vanish or get reduced when more partial waves will be included.

Let us compare the collision delays found from different potentials. All members from the set of Bonn potentials provide nearly identical results. There is also only a minor difference between the Paris and the Bonn potentials. The strongest difference appears between the separable Paris potential and the other for the back scattering. Nevertheless, one can conclude that on the scale of precision of recent theory of heavy ion reactions, all potentials are equally acceptable.

B. Hard-sphere displacement

The hard-sphere displacement $\overline{\Delta_{\rm HS}}$ is plotted in Fig. 3. Unlike the collision duration, the displacement is regular at low energies going to zero for $|\kappa|\to 0$. This is caused by the dominant contribution of the S wave in this region. When the S wave dominates, the hard-sphere displacement simplifies as $\overline{\Delta_{\rm HS}}=-\frac{1}{2}\sin\theta/2\,\mathrm{Im}(1/T_0)(\partial T_0/\partial|\kappa|)$. From analyticity follows that at small momenta the T matrix depends on $|\kappa|^2$, therefore $\partial T_0/\partial|\kappa|\propto|\kappa|$ and vanishes for $|\kappa|\to 0$.

Again, there is a strong and irregular angular dependence. The angular variation of $\overline{\Delta_{\rm HS}}$, visible for deflection angles $\theta=60°,90°,120°$, clearly shows that the model of hard spheres is not adequate for any energy region, because it yields the angle-independent length of displacement. It is interesting that for the nonseparable potentials the effective hard sphere is very small at the back scattering, $\theta=180°$, in spite of the maximum of the factor $\sin\theta/2$. The negative value of the length $\overline{\Delta_{\rm HS}}$ at $\theta=120°$ shows that the nonlocal corrections to the nucleon-nucleon collision cannot be estimated from the hard core of the nucleon-nucleon potential. If the effect of the real hard core would dominates the nonlocality, the length of displacement is expected to be positive and equal twice the radius of the core.

Finally, the perpendicular scattering has a singularity at energy 80 MeV. Similarly to the singularity of the collision duration, the enormous values of nonlocal corrections at this point are not dangerous for the validity of the kinetic equation, because they appear due to vanishing differential cross sections. Traces of this singularity can be seen also for scat-

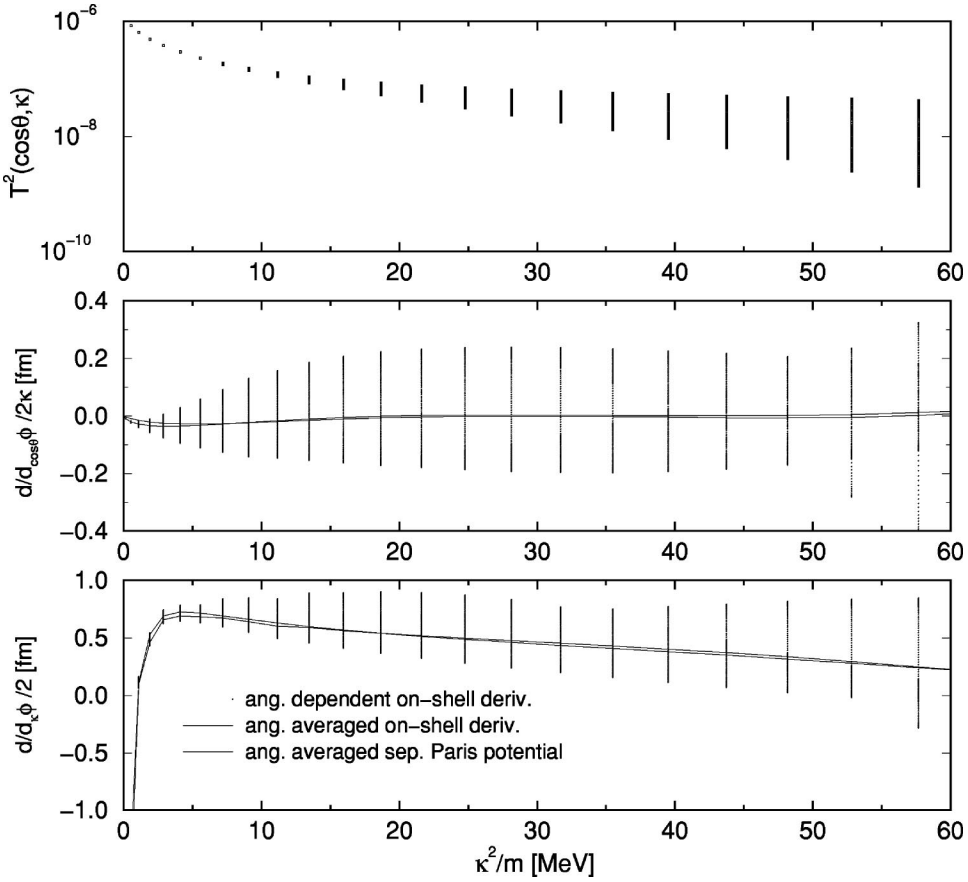

FIG. 5. The effective displacement as a function of the deflection angle and the kinetic energy κ^2/m in the barycentric coordinate system. The columns of dots show the spread of components with deflection angle. The lines show the angle-averaged values. The amplitude of the T matrix is presented in the top section to indicate the weight of individual processes. The orthogonal component $\overline{\Delta_\perp} \equiv d/d_{\cos\theta}\phi$ shown in the middle section, has appreciably smaller values than the parallel component $\overline{\Delta_\parallel} \equiv d/d_\kappa\phi/2$ shown in the bottom section.

tering at close angles $\theta=60°$ and $\theta=120°$.

The nonseparable potentials yield quite close values of the hard-sphere displacement. Certain difference between the Bonn and Paris potentials appears at low energies for $\theta=60°$. Recent precision of heavy-ion-reaction simulations, however, does not allow us to distinguish such a detail. Strong differences result only between the separable and nonseparable potentials, in particular, for the back scattering.

C. Rotational displacement

The rotational displacement $\overline{\Delta_\phi}$ is plotted in Fig. 4. In the limit of low energies it vanishes from a similar reason as the hard-sphere displacement. When the S wave dominates, the rotational displacement simplifies as $\overline{\Delta_\phi}=\frac{1}{2}\cos\theta/2\,\mathrm{Im}(1/T_0)(\partial T_0/\partial|\kappa|)$ which goes to zero as $|\kappa|\to 0$.

Except for the low-energy region, the rotation displacement has a number of features similar to the collision duration, at least for $\theta=90°$ and $\theta=120°$. For the perpendicular scattering, the $1/x$ discontinuity appears at 80 MeV. The step for $\theta=120°$ at 40 MeV is also similar including the shoulder at 120 MeV. The velocity of particles in the barycentric framework for 80 MeV is about a half of the velocity of light, which crudely corresponds to the coefficient with which the discontinuity of the collision duration scales on the discontinuity of the rotational displacement. We are not aware of the real reason for this similarity, nevertheless, it is noteworthy that for a collision of classical particles the rotational displacement is also proportional to the collision duration, because the longer the collision lasts the more the colliding pair can revolve. For instantaneous collisions, no rotational displacement appears due to a continuity of classical trajectories, see Fig. 1. In contrast, the hard-sphere displacement is generally nonzero for instantaneous collisions as it is the case for the true hard spheres. Small correlation between Δ_t and Δ_{HS} is also confirmed by the numerical results, at least Figs. 2 and 3 do not show similar features.

Except for singularities, which are invisible due to the small differential cross section, the typical values of the rotational displacement are slightly smaller but close to the hard-sphere displacement. In Refs. [2–4] the rotational displacement has not been assumed. The found numerical values do not justify this neglect.

D. Wigner collision delay

At the low-energy region $|\kappa|^2/m<30$ MeV, the collision duration becomes a sizable correction while the displacements are rather small. This energy domain is important for heavy ion collisions at medium energies, it is thus worthy to test the validity of the approximation by the Wigner collision delay in more details.

To make a comparison of the noninstantaneous and the nonlocal corrections easier, we express both in the form of displacements which enter the simulation codes, as has been done in Ref. [6]. Assuming that the collision event is identified at the instant of the closest approach of particles, the total effective displacement in the direction of outgoing relative momentum $\Delta_\parallel=(\kappa_f/|\kappa|)\overline{\Delta_\parallel}$, has the length

$$\overline{\Delta_\parallel}=\mathrm{Im}\left[\frac{1}{T}\sum_l P_l\left(\frac{\partial T_l}{\partial\Omega}\frac{2|\kappa|}{m}+\frac{\partial T_l}{\partial|\kappa|}\right)\right]$$
$$=\frac{2|\kappa|}{m}\mathrm{Im}\left[\frac{1}{T}\sum_l P_l\left(\frac{\partial T_l}{\partial\Omega}+\frac{\partial T_l}{\partial(|\kappa|^2/m)}\right)\right]=\frac{2|\kappa|}{m}\Delta_t^W. \tag{15}$$

This displacement combines the collision duration, the final relative displacement $\frac{1}{2}(\Delta_4-\Delta_3)=\Delta_{\mathrm{HS}}+\Delta_\phi$ projected on the direction of the final momentum κ_f, and the initial relative displacement $\frac{1}{2}\Delta_2=\Delta_{\mathrm{HS}}-\Delta_\phi$ projected on the direction of the initial momentum κ. For details of the instantaneous approximation see Ref. [6]. The same displacement results when one derives the nonlocal correction from the Wigner collision delay Δ_t^W.

The displacement perpendicular (inside the collision plane) to the direction of the outgoing relative momentum has a length

$$\overline{\Delta_\perp}=-\frac{\sin\theta}{|\kappa|}\mathrm{Im}\left[\frac{1}{T}\sum_l P_l' T_l\right]. \tag{16}$$

This perpendicular component is neglected within the approximation derived from the Wigner collision delay.

Numerical values of these two contributions are compared in Fig. 5. The dots in the vertical line show a spread of values due to the angular dependence, the curves show values averaged over deflection angles with the weight given by the differential cross section displayed in the top section. The parallel component, shown in the bottom section, has a typical value of 0.5 fm. The negative large values below 3 MeV can be ignored since corresponding processes have very small rates due to the Pauli blocking. The perpendicular component, shown in the middle section, has about three-times smaller values, moreover it tends to average out. These results confirm that the approximation based on the Wigner collision delay as proposed by Danielewicz and Pratt [4] is suitable for the nuclear matter at low energies.

V. SUMMARY

The numerical values of the collision duration and displacements of particles in a binary collision are comparable with typical time and space scales in reacting heavy ions. This shows that noninstantaneous and nonlocal treatments of binary collisions in simulations of heavy ion reactions are desirable.

The found collision duration and displacements slightly depend on the employed interaction potential. The differences are, however, too small to be detectable within the accuracy of recent realistic simulations. Stronger deviations have appeared for the separable potential at higher energies. This was expected, since the separable approximation is suited for the low-energy region only.

We have tested the approximations of nonlocal corrections adopted or suggested in print. The energy and angular dependence of the duration and displacements do not justify the hard-sphere model. On the other hand, the approximation by the Wigner collision delay covers the dominant nonlocal corrections in the low-energy region.

ACKNOWLEDGMENTS

The authors are grateful to S. Köhler for stimulating discussions. A. Schnell is thanked for the code of separable potential. This work was supported from the Czech republic, GACR Nos. 202960098 and 202960021 and GAASCR No. A1010806, and Germany, BMBF No. 06R0884, and the Max-Planck Society.

[1] E. C. Halbert, Phys. Rev. C **23**, 295 (1981).
[2] R. Malfliet, Nucl. Phys. **A420**, 621 (1984).
[3] G. Kortemeyer, F. Daffin, and W. Bauer, Phys. Lett. B **374**, 25 (1996).
[4] P. Danielewicz and S. Pratt, Phys. Rev. C **53**, 249 (1996).
[5] V. Špička, P. Lipavský, and K. Morawetz, Phys. Lett. A **240**, 160 (1998).
[6] K. Morawetz, V. Špička, P. Lipavský, G. Kortemeyer, Ch. Kuhrts, and R. Nebauer, Phys. Rev. Lett. (to be published), nucl-th/9810043.
[7] M. Schmidt, G. Röpke, and H. Schulz, Ann. Phys. (N.Y.) **202**, 57 (1990).
[8] M. L. Goldberger and K. M. Watson, *Collision Theory* (Wiley, New York, 1964).
[9] R. Machleidt, Adv. Nucl. Phys. **19**, 189 (1989).
[10] R. Machleidt, in *Computational Nuclear Physics*, edited by K. Langanke, J. A. Maruhn, and S. E. Koonin (Springer, New York, 1993), Vol. 2.
[11] M. Lacombe *et al.*, Phys. Rev. C **21**, 861 (1980).
[12] J. Heidenberger and W. Plessas, Phys. Rev. C **30**, 1822 (1984).